2025 IEEE/SICE International Symposium on System Integration (SII)
January 21-24, 2025, Munich, Germany

Servo-Driven Flapping-Wing Aerial Vehicle (FWAV): Payload Capacity and Navigation Performance

Muhammad Labiyb Afakh[1], Azhar Aulia Saputra[1], Hidaka Sato[1], Kazuyoshi Wada[1] and Naoyuki Takesue[1]

Abstract— **In the current situation, environmental monitoring and disaster mitigation become a concern. There are many developed robot in different type for enviromental issue, but some robot has limitation on coverage area. To solve that problem, several researcher also developed FWAV that has potential on environment monitoring application. This study aims to enhance the potential of Flapping Wing Aerial Vehicles (FWAVs) for wider implementation in these fields. While most FWAVs traditionally use a single actuator, leading to manufacturing and design complexity, recent trends show a shift towards servo-driven mechanisms due to their enhanced capabilities. We achieve modularity through a design that allows for easy assembly and disassembly of main wings, tail, and hardware components. Performance enhancements are realized through the implementation of a square wave pattern as the input signal for flapping motion, which outperforms the common sinusoidal wave pattern as input signal. By adjusting the center of gravity and flapping parameters, we demonstrate the FWAV's potential to carry payloads of up to 100 grams which is almost 28% of its weight, suitable for small-scale environmental monitoring missions. Additionally, we implement a collision avoidance system to enhance the FWAV's ability to navigate safely in complex environments.**

I. Introduction

In the current situation, environmental monitoring and disaster mitigation become a concern. Implementation of aerial vehicles to monitor the environment have been studied. There are many developed robot in different type for enviromental issues, such as: legged robot [1], [2], mobile robot [3]. However, this type of robot has limitation on the coverage area. Therefore flying robot become on of the solution to coverage larger area [4]. A study demonstrated implementation of quadcopter in Antarctic environmental research [5].

There are several researcher developed FWAV that has potential on environment monitoring application [6], [7], [8]. FWAV has advantages in low surrounding effect such as noise, wind, and shape. Zufferey *et al.* has proposed Eagle-inspired Flapping-wing robot E-Flap, a 510 g novel design capable of a 100% of payload [6]. They use single actuator for driving the flapping wing. In other hand, Dove *et al.*, proposed flexible wing design, the flapping mechanism design, and the on-board avionics development. The proposed robot has a mass of 220 g and a wingspan of 50 cm [7].

In the recent studies, most of FWAV designs have relied on a single actuator for driving the flapping motion of the wings. In our previous FWAV design, we used single actuator with gear compliant [9]. However, this structure may cause manufacturing and design complexity [10] implied the increasing of weight and size. Recent research explored a hybrid actuation mechanism between fast-rotating propeller and flapping mechanism have been demonstrated[11]. It enables wide implementation. Despite these innovations, structural fragility remains a challenge for FWAVs, as they are more prone to damage compared to other aerial vehicles, especially as size increases.

Currently, there is a growing trend toward servo-driven FWAVs due to their modularity and improved wing control. The servo-driven design allows more flexible and adaptive wing motions to achive the better performance. The modularity of servo-driven mechanisms, as demonstrated by[12], offers versatility in design and function. Huang *et al.* have further shown that servo-driven mechanisms substantially enhance the performance of flapping wing robots by allowing for more nuanced and responsive wing movements[13]. A servo-driven structure offers the advantage of modularity, but this design choice can potentially give an indirect impact on its performance due to the additional mass of servo components contributing to the robot's overall weight. Choosing the best servo motor to meet the desired performance can also be challenging on this structure.

Another fascinating performance mimicking a real bird locomotion are also demonstrated in the study of FMAV. An ornithopter that can perch on a branch autonomously represents remarkable progress [14]. This capability not only conserves energy but also opens up possibilities for extended environmental monitoring and mapping. To improve FMAV agility, a study on a servo-driven flapping with jumping takeoff has been conducted [15]. While several FMAVs have demonstrated the ability to carry payloads of up to 500 grams, there is a current gap in research regarding servo-driven FWAVs specifically designed for payload capacity. This presents an opportunity for future studies to explore the development of servo-driven FWAVs optimized for carrying payloads, potentially expanding their practical applications.

During performing a mission, FWAVs should have safety mechanism to reduce the possibility of crashes. A study using event based camera shows robust dynamic sensing and avoidance[16]. Another obstacle avoidance that is quite lightweight and low-cost sensor are utilized [17]. Since the robot is a hovering type, the challenge of minimum robot velocity to fly is not an issue. For forward-flight FWAV, it is quite challenging because the robot needs to achieve certain speed to produce enough thrust. Our previous study shows that a payload presents a significant challenge

[1]Department of Mechanical Systems Engineering, Graduate School of Systems Design, Tokyo Metropolitan University, Japan. afakh-muhammad-labiyb@ed.tmu.ac.jp, ntakesue@tmu.ac.jp

Fig. 1: OrnibiBot 3.0.

for FWAVs. An observation was conducted to identify the optimal parameters required for FWAV performance [18]. This study contributes to :

- Modular and durable design to make it easy to carry and reduces the maintenance complexity .
- Fly with payload.
- A low-cost and lightweight obstacle avoidance.

The paper is organized as follows. Section II presents the proposed robot structure and system. Then, Section III shows experimental results including static force measurement, free flight, carrying payload and collision avoidance. Finally, Section IV shows the conclusion of the proposed model.

II. Developed Robot

A. Mechanical Design

Figure 1 shows the whole robot structure. The inner wing is design to have good rigidness and the outer wing is more flexible to improve the efficiency and force generated. Table.I show the detail information developed robot. To generate a flapping motion, Futaba CT-700 servo motors are utilized to enable robust performance. By finding the proper wing geometry and weight, it allows the robot to perform a good flight. The mass of the wing significantly impacts the efficiency and effectiveness of flapping flight due to the maximum inertia that can be handled by servo motor.

The previous mechanism was not able to fly due to center of gravity, weight and wing structure. To reduce the weight of robot on the rear side, the way of robot to turn left and right is enabled by changing flapping offset for each wing to generate yaw torque as studied on [13]. Since the goal is to carry a payload, its center of gravity is located in a half-of wing chord length so it is expected to help the robot to generate negative pitch moment or nose up. It will increase the potential of robot to generate larger lift. Drag acts to the front side of robot can be a problem. To minimize that problem, a shaped-sponge is attached on the front side. It can help the robot to flight better.

B. System

In the first scenario, to control the FWAV with a minimum hardware requirement that is easy to find, an XIAO ESP32S3 is utilized. It allows to control the robot via WiFi over UDP communication. The target position of the robot's wing $\theta(t)$ is governed by Equations (1) and (2), which define sinusoidal and square wave motion patterns. The calculated $\theta(t)$ in degrees is converted to actuator units through linear mapping and transmitted via serial SBUS protocol to the actuator. A, β, T, t denote the flapping amplitude, offset, period, time for each period. When the robot can fly well, the second scenario of system is proposed to support collision avoidance. Enhancing the performance is also proposed by implementing collision avoidance. An 8x8 time of flight (ToF) sensor, VL53L5CX, is selected to observe the obstacle on the flight path. It requires more computational resources on microcontroller level.

TABLE I: Robot specifications

Wingspan	1.5m
Chord Length	0.3m
Flapping Frequency	$5-7$Hz
Input voltage	8.4 V
Weight	350 grams

TABLE II: Average thurst $\overline{F_x}$ and lift $\overline{F_z}$ of sinusoidal and square patterns.

Pattern (Frequency)	$\overline{F_x}$	$\overline{F_z}$
Sinusoidal (4Hz)	3.13N	-0.122N
Square (4Hz)	2.97N	-0.11N
Sinusoidal (5Hz)	2.69N	-0.01N
Square (5hz)	2.68N	0.14N
Sinusoidal (6Hz)	2.53N	-0.007N
Square (6hz)	2.39N	0.27N

$$\theta(t) = A \cdot \sin\left(\frac{2\pi t}{T}\right) + \beta \tag{1}$$

$$\theta(t) = A \cdot \mathrm{sgn}\left(\sin\left(\frac{2\pi t}{T}\right)\right) + \beta \tag{2}$$

Figure 2 shows how the system is constructed to achieve the goal of this study to perform collision avoidance by utilizing 2 microcontrollers. To handle that task, a Teensy 4.0 which is a small size microcontroller with high clock speed around 600Hz is utilized. Input signal to the actuator is interpolated and sent by a Teensy 4.0. It also handles the visual information and processing the approach to avoid the obstacle. The visual information from ToF will control the maneuver of the robot to avoid the collison. IMU BNO055 and BMP280 are also utilized to provide some information on the performance while performing collision avoidance and sending the data to the PC over UDP.

III. Experimental Results

To show the effectiveness of the proposed model, we have conducted following experiments: A) Static force measurement B) Flight experiments C) Carrying payload experiments D) Collision avoidance experiments.

A. Static Force measurement

To clarify the performance of FWAV, the generated force is observed by attaching the robot on FWAV on a Leptrino,

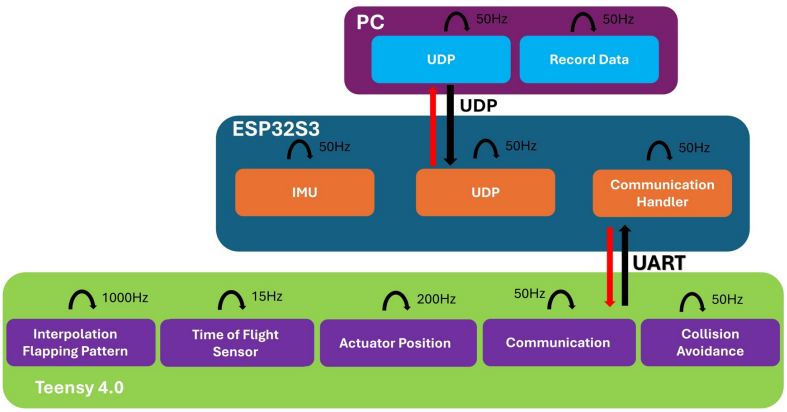

Fig. 2: System architecture

a 6-DoF force sensor, that is fixed on a platform. The front side of robot is connected and tighted to a holder support that made by 3D printed part. Then, that holder support is directly connected to the force sensor. In this experiment, the angle of attack (AoA) is set to 0 degree. It helps to know the minimum lift force when the robot perform level flight. Also, microcontroller and battery are not attached on the robot during this experiment.

Figure 3 shows the thrust and lift generation in FWAV. It shows that sinusoidal pattern generates more higher thurst than square pattern when we look at the area under the curve. It equals to the previous work [18]. The generated force is also selected based on that previous work. To dive more on this data, we provide the calculation on the average thurst $\overline{F_x}$ and lift $\overline{F_z}$ on Table. II. It shows that the thrust tends to decrease and lift tends to increase when we increase the flapping frequency. The square wave pattern can produce more overage on lift. The potential improvement can also be achieved if the center of gravity is shifted to the sufficient position to generate sufficient AoA during flight.

B. Flight Experiment

To clarify the result of static force measurement experiment, flight experiment is conducted. Figure 4 shows the performance of robot during free flight. The takeoff phase is done by launch it by hand. The robot is proved to fly around a minute for an indoor flight. The robot can also perform a good flight for an outdoor flight. The performance of robot to fly stablecan be achieved by set the flapping frequency around 5Hz and the flapping amplitude is set to 70 degrees. To help the robot generating a positive angle of attack or nose up, its tail is set to 30 degree which is pointed to upside. The positive angle of attack will enchance the generated lift so the robot can maintain its altitude or fly higher. Smooth landing also can be perform by decreasing the flapping frequency gradually. It also can be coupled by setting the tail to negative position which is pointed to the downside.

The robot can easily turn by changing the offset β for each actuator and generates yaw moment. By adjusting the offset value, the robot can perform smooth or rapid turning. From the flight experiment, it prove that the square wave pattern enables the robot to fly on a certain performance compared to sinusoidal wave pattern. It also clarified on another studies on servo-driven utilizing the square wave pattern for flight [15] [19]. According to the previous study [18], the higher amplitude can also generate the force. It can be clarified from this experiment, when the amplitude is set to 60 and 70 degree, the 70 degree can produce more force even though that actual position of actuator could not reach that desired position.

C. Carrying Payload Experiment

To evaluate the potential for widespread implementation, the robot's flight capabilities were assessed under various payload conditions. A series of tests were conducted using calibrated weights as payloads. Five distinct payload configurations were examined: 0 g (no payload), 20 g, 50 g, 70 g, and 100 g. These precisely measured weights were selected to provide a comprehensive understanding of the robot's performance across a range of payload masses, from unloaded to maximum capacity.

To track its position an Optitrack Flex 13, a motion capture camera system, is utilized. A reflective marker is attached in front of the robot. Figure 5 shows the performance of robot to carry payload during flight. From the experimental data, the purple line shows that robot is not able to fly while carrying a 100 grams payload with 5Hz flapping frequency. After the adjustment of flapping frequency to 6Hz and refering to the result of static measurement thrust, the issue can be solved because the robot can achieve sufficient lift to carry that payload, but it may requires more power and decrease the turning performance.

The maximum performance of robot in generating force affects its payload-carrying capability. In order to carry up to 500 grams payload like E-Flap [6], a high-performance servo motor should be utilized, but finding or developing suitable ones presents a significant challenge. Compared to a single actuator, the tradeoff of using servo is that the gap between actual and desired angle will be larger when we try to increase the flapping frequency due to the servo performance. It will be a challenge for servo-driven FWAV structure. This challenge becomes more significant as higher

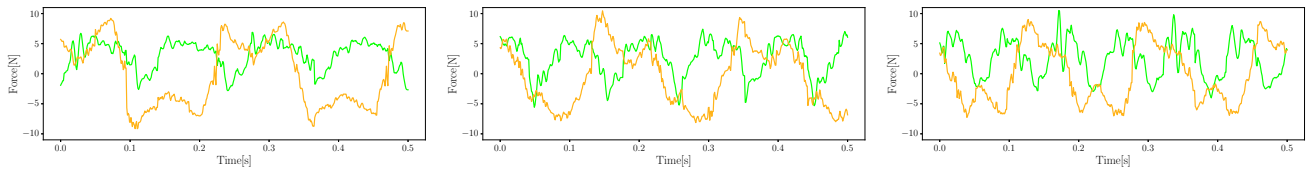

(a) Sinusoidal 4Hz (b) Sinusoidal 5Hz (c) Sinusoidal 6Hz

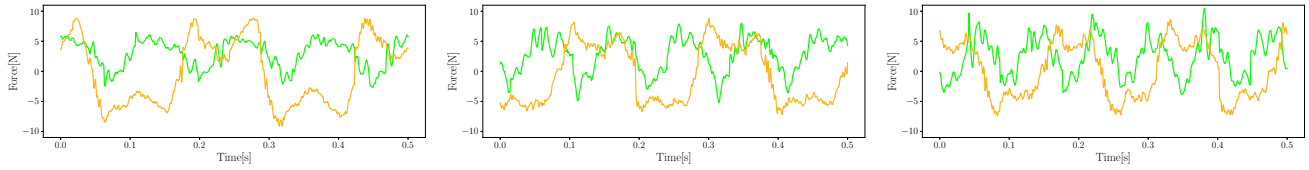

(d) Square 4Hz (e) Square 5Hz (f) Square 6Hz

Fig. 3: The green and orange line represent the generated thurst and lift by the robot.

Fig. 4: Snapshot of free flight in 14 secs.

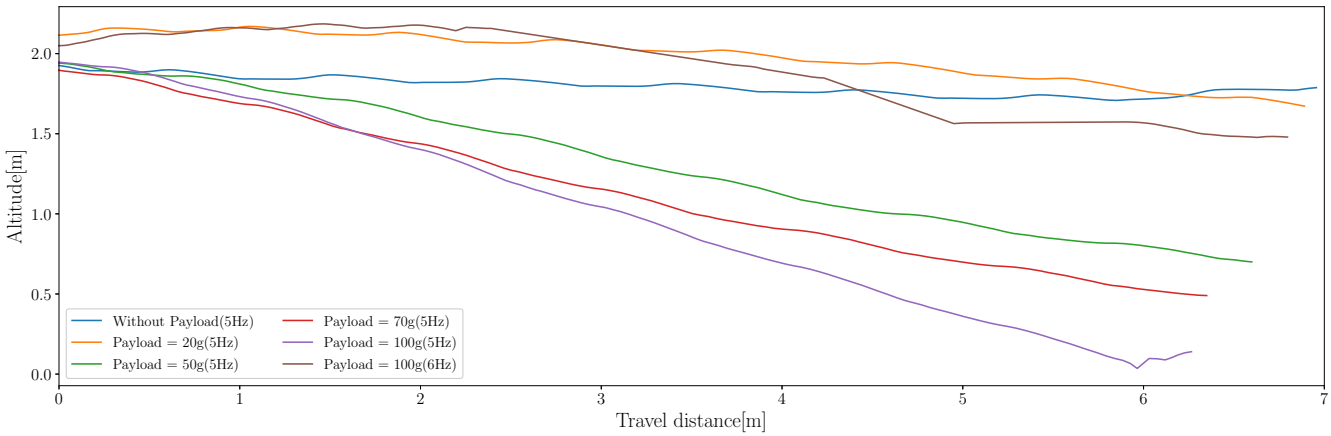

Fig. 5: Flight with payload experiment.

payload requires greater lift and thrust generation, which is difficult to achieve when there is a substantial gap between the actual and desired wing positions.

D. Collision Avoidance Experiment

To enhance the robustness of robot while performing a task, a low-cost obstacle avoidance is implemented. Utilizing the VL53L5CX ToF sensor which located on the middle of front side, collision object is estimated. The information for each pixel will be updated in 15Hz sampling rate. Considering the velocity and turning performance of robot, the closest distance d_{safe} is set to 1.2 meter. The maximum distance for this ToF is around 4m with the minimum distance can be. It will estimate the free area O_{ij} for each pixel information D_{ij}.

$$O_{ij} = \begin{cases} 1 & \text{if } D_{ij} < d_{safe} \\ 0 & \text{otherwise} \end{cases} \tag{3}$$

Fig. 6: Modified robot with ToF sensor.

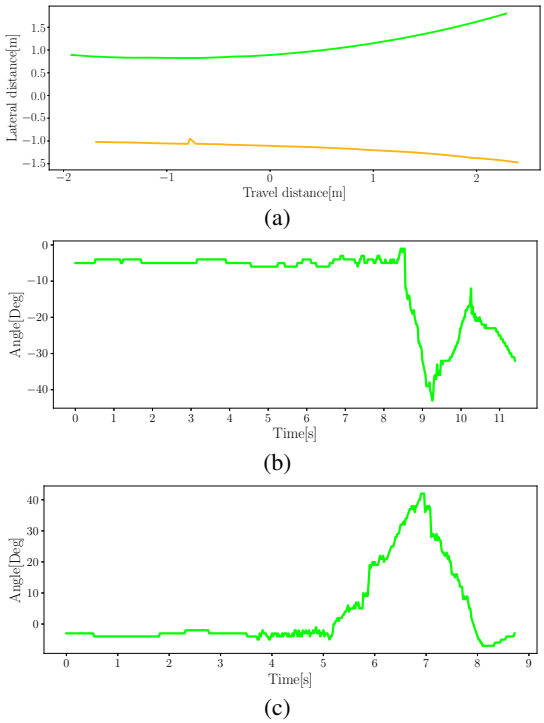

Fig. 7: (a) visualizes the trajectory of the robot during performing collision avoidance. (b) and (c) are the actual roll angle of the robot during flight and avoiding the obstacle.

After the free or obstacle area information is gathered, it will be counted into left C_{left} and right C_{right} obstacle position.

$$C_{left} = \sum_{i=1}^{n} \sum_{j=1}^{n/2} O_{ij} \tag{4}$$

$$C_{right} = \sum_{i=1}^{n} \sum_{j=n/2+1}^{n} O_{ij} \tag{5}$$

The origin of motion capture camera is close to the obstacle which is approximately 0.3 to 0.5m before the obstacle. A pillar that has 1m diameter becomes an obstacle that should be avoided by the robot. Fig.7(a) shows the trajectory of the robot while performing collision avoidance. The green line shows how the robot turning left to avoid the obstacle on the right side. On the other hand, the orange line represents the trajectory of the robot to avoid the obstacle located on the left side. Figure 7(b) shows how the robot responses by generating a negative rolling angle. Figure 7(c) shows the robot generating positive roll moment to turn right from five second to seven second. After the object has been passed or the area in front of the robot is free, the robot will try to recover to the idle position that can be seen from seven to eight second. It shows the capability to avoid a collision which becomes a basic requirement of robot for outdoor implementation to minimize the chance of hitting a human or obstacle during flight.

IV. Conclusion

This paper presents servo-driven flapping-wing aerial vehicles (FWAV) that can achieve capability to carry payload and enabling collision avoidance during flight. It becomes a challenge for a servo-driven FWAV. In many cases, single actuator with gear reduction and lever crank mechanism can achieve it easily. A combination of balance for some parameters like actuator performance, wing and tail structure, flapping parameter and cente of gravity play important role to achieve this goal.

Modularity can be achieved by assembling and disassembling the main wing, tail, and hardware. In term of performance, square wave pattern can outperform sinousidal wave pattern. The flight test also prove that square wave pattern is the solution to enable fascinating performance even though the actuator could not achieve desire position.

We demonstrated the FWAV's capability to carry a payload of up to 28% of its own weight. For instance, with a total robot weight of 360 grams, it can carry up to 100 grams of additional payload for a small mission such as environmental monitoring. From the collision avoidance experiment, it shows a possible implementation, but it will be better to find a proper ToF or depth camera sensor that can recognize the collision object in several meters longer than the current ToF sensor. As for the future work, the robustness and realibility of collision avoidance will be improve to achieve aggresive flight or mission flight.

ACKNOWLEDGMENT

This work was supported by JST SPRING, Grant Number **JPMJSP2156** and TMU local 5G research support.

References

[1] M. Hutter, C. Gehring, D. Jud, A. Lauber, C. D. Bellicoso, V. Tsounis, J. Hwangbo, K. Bodie, P. Fankhauser, M. Bloesch *et al.*, "Anymal-a highly mobile and dynamic quadrupedal robot," in *2016 IEEE/RSJ international conference on intelligent robots and systems (IROS)*. IEEE, 2016, pp. 38–44.

[2] A. A. Saputra, N. Takesue, K. Wada, A. J. Ijspeert, and N. Kubota, "Aquro: A cat-like adaptive quadruped robot with novel bio-inspired capabilities," *Frontiers in Robotics and AI*, vol. 8, p. 562524, 2021.

[3] K. Nagatani, A. Yamasaki, K. Yoshida, and T. Adachi, "Development and control method of six-wheel robot with rocker structure," in *2007 IEEE International Workshop on Safety, Security and Rescue Robotics*. IEEE, 2007, pp. 1–6.

[4] J. A. Preiss, W. Honig, G. S. Sukhatme, and N. Ayanian, "Crazyswarm: A large nano-quadcopter swarm," in *2017 IEEE International Conference on Robotics and Automation (ICRA)*. IEEE, 2017, pp. 3299–3304.

[5] A. Tovar-Sánchez, A. Román, D. Roque-Atienza *et al.*, "Applications of unmanned aerial vehicles in antarctic environmental research," *Scientific Reports*, vol. 11, p. 21717, 2021.
[6] R. Zufferey, J. Tormo-Barbero, M. M. Guzmán, F. J. Maldonado, E. Sanchez-Laulhe, P. Grau, M. Pérez, J. Á. Acosta, and A. Ollero, "Design of the high-payload flapping wing robot e-flap," *IEEE Robotics and Automation Letters*, vol. 6, no. 2, pp. 3097–3104, 2021.
[7] W. Yang, L. Wang, and B. Song, "Dove: A biomimetic flapping-wing micro air vehicle," *International Journal of Micro Air Vehicles*, vol. 10, no. 1, pp. 70–84, 2018.
[8] A. Ramezani, X. Shi, S.-J. Chung, and S. Hutchinson, "Bat bot (b2), a biologically inspired flying machine," in *2016 IEEE International Conference on Robotics and Automation (ICRA)*. IEEE, 2016, pp. 3219–3226.
[9] M. L. Afakh, T. Sato, H. Sato, and N. Takesue, "Development of flapping robot with self-takeoff from the ground capability," in *2021 IEEE International Conference on Robotics and Automation (ICRA)*. IEEE, 2021, pp. 321–327.
[10] M. L. Afakh, H. Sato, and N. Takesue, "Study towards a flapping robot maintaining attitude during gliding," *International Journal on Advanced Science, Engineering and Information Technology*, vol. 13, p. 681–687, Apr. 2023.
[11] S. Gupta, K. P. Rithwik, K. Prashanth, A. Ashe, and H. Kandath, "Design and analysis of a modular flapping wing robot with a swappable powertrain module," in *2024 IEEE International Conference on Mechatronics and Automation (ICMA)*, 2024, pp. 323–328.
[12] I. D. de-los Rios, A. Suarez, E. Sanchez-Laulhe, I. Armengol, and A. Ollero, "Winged aerial robot: Modular design approach," in *2021 IEEE International Symposium on Safety, Security, and Rescue Robotics (SSRR)*, 2021, pp. 190–195.
[13] H. Huang, W. He, J. Wang, L. Zhang, and Q. Fu, "An all servo-driven bird-like flapping-wing aerial robot capable of autonomous flight," *IEEE/ASME transactions on mechatronics*, vol. 27, no. 6, pp. 5484–5494, 2022.
[14] R. Zufferey, J. Tormo-Barbero, D. Feliu-Talegón, S. R. Nekoo, J. Ángel Acosta, and A. Ollero, "How ornithopters can perch autonomously on a branch," *Nature Communications*, vol. 13, p. 7713, 2022. [Online]. Available: https://doi.org/10.1038/s41467-022-35356-5
[15] W. Yan, G. Chen, Z. Zhang, and H. Wang, "A meter-scale ornithopter capable of jumping take-off," in *2024 IEEE International Conference on Robotics and Automation (ICRA)*, 2024, pp. 1583–1589.
[16] J. P. Rodríguez-Gómez, R. Tapia, M. d. M. G. Garcia, J. R. M.-d. Dios, and A. Ollero, "Free as a bird: Event-based dynamic sense-and-avoid for ornithopter robot flight," *IEEE Robotics and Automation Letters*, vol. 7, no. 2, pp. 5413–5420, 2022.
[17] C. De Wagter, S. Tijmons, B. D. W. Remes, and G. C. H. E. de Croon, "Autonomous flight of a 20-gram flapping wing mav with a 4-gram onboard stereo vision system," in *2014 IEEE International Conference on Robotics and Automation (ICRA)*, 2014, pp. 4982–4987.
[18] M. L. Afakh, H. Sato, and N. Takesue, "Performance Evaluation and Wing Deformation Analysis of Flapping-Wing Aerial Vehicles with Varying Flapping Parameters and Patterns," *Journal of Robotics and Mechatronics*, vol. 36, no. 5, 2024, in press.
[19] H. Huang, W. He, J. Wang, L. Zhang, and Q. Fu, "An all servo-driven bird-like flapping-wing aerial robot capable of autonomous flight," *IEEE/ASME Transactions on Mechatronics*, vol. 27, pp. 5484–5494, 2022.